Dilated cardiomyopathy caused by tissue-specific ablation of SC35 in the heart

Jian-Hua Ding[1], Xiangdong Xu[1], Dongmei Yang[2], Pao-Hsien Chu[3,4], Nancy D Dalton[3], Zhen Ye[1], Joanne M Yeakley[1,5], Heping Cheng[2], Rui-Ping Xiao[2], John Ross Jr[3], Ju Chen[3] and Xiang-Dong Fu[1,*]

[1]Department of Cellular and Molecular Medicine, University of California at San Diego, La Jolla, CA, USA, [2]Laboratory of Cardiovascular Science, Gerontology Research Center, NIA, NIH, Baltimore, MD, USA and [3]Department of Medicine and Institute of Molecular Medicine, University of California at San Diego, La Jolla, CA, USA

Many genetic diseases are caused by mutations in *cis*-acting splicing signals, but few are triggered by defective *trans*-acting splicing factors. Here we report that tissue-specific ablation of the splicing factor SC35 in the heart causes dilated cardiomyopathy (DCM). Although SC35 was deleted early in cardiogenesis by using the MLC-2v-Cre transgenic mouse, heart development appeared largely unaffected, with the DCM phenotype developing 3–5 weeks after birth and the mutant animals having a normal life span. This nonlethal phenotype allowed the identification of downregulated genes by microarray, one of which was the cardiac-specific ryanodine receptor 2. We showed that downregulation of this critical Ca^{2+} release channel preceded disease symptoms and that the mutant cardiomyocytes exhibited frequency-dependent excitation–contraction coupling defects. The implication of SC35 in heart disease agrees with a recently documented link of SC35 expression to heart failure and interference of splicing regulation during infection by myocarditis-causing viruses. These studies raise a new paradigm for the etiology of certain human heart diseases of genetic or environmental origin that may be triggered by dysfunction in RNA processing.

Introduction

Pre-mRNA splicing is essential for gene expression in mammalian cells as most genes contain introns, which need to be precisely removed in the nucleus by the splicing machinery (Burge *et al*, 1999). In addition, many transcripts are alternatively spliced to generate functionally distinct proteins from the same pre-mRNA, thereby increasing the complexity of the proteome in eucaryotic cells (Black, 2000). The functional integrity of the splicing machinery is crucial for normal developmental and tissue-specific control of gene expression, and human diseases have been increasingly attributed to the disruption of splicing regulation (Faustino and Cooper, 2003). Strikingly, an earlier survey indicates that nearly 15% of disease-causing mutations disrupt conserved splicing signals, resulting in inactivation or downregulation of affected genes (Krawczak *et al*, 1992). Because this earlier survey was based on constitutive splicing signals in introns, the scope of mutations that cause diseases via the splicing pathway is probably underestimated. As highlighted in a recent review, many disease-causing mutations in protein-coding exons may affect splicing, instead of protein function as commonly assumed (Cartegni *et al*, 2002). This is because many exonic sequence motifs also function as splicing enhancers, which are widely present in both constitutive and alternative exons (Mayeda *et al*, 1999; Schaal and Maniatis, 1999).

While diseases triggered by mutations in *cis*-acting elements are well known, little was known about disease-causing *trans*-acting splicing factors until recently. Extensive biochemical studies show that exonic splicing enhancers are recognized by a variety of RNA interacting factors. One of the best characterized classes of splicing enhancer recognition factors is the serine/argininerich (SR) family of splicing factors, which contain one or two RNA recognition motifs (RRMs) and a signature motif enriched in arginine/serine dipeptide repeats (RS domain) (Graveley, 2000). SC35 is a prototypical SR protein originally identified to be an essential splicing factor involved in multiple steps of spliceosome assembly (Fu and Maniatis, 1990; Vellard *et al*, 1991), and later found to affect alternative splicing (Fu *et al*, 1992). Such a dual function is true with all SR proteins, which are thus believed to play roles in both constitutive and regulated splicing. Although SR proteins are collectively essential for splicing, different SR proteins exhibit unique substrate specificities by recognizing distinct splicing enhancer elements in pre-mRNA (Graveley, 2000).

In contrast to the wealth of knowledge of SR proteins and related splicing regulators at the biochemical level, relatively little is known about their functions *in vivo* and how they might contribute to disease. One of the major hurdles to *in vivo* studies is that null mutations in SR proteins appear to cause cell and embryonic lethality. This was first reported with the SR protein ortholog B52 in the fly (Ring and Lis, 1994). Gene targeting of the SR protein SF2/ASF in a chicken B-cell line (DT40) resulted in cell lethality (Wang *et al*, 1996). Deletion of SRp20 in the mouse caused embryonic lethality at the blastocyst stage (Jumaa *et al*, 1999). These experiments give rise to a general impression that SR proteins perform fundamental functions crucial for cell viability. However,

inactivation of individual SR proteins by RNAi in *Caenorhabditis elegans* had little effect on development, except that inactivation of SF2/ASF induced a late embryonic lethality (Longman *et al*, 2000).

Our laboratory previously reported a gene-targeting study with SC35 in T cells, which causes defects in T cell maturation (Wang *et al*, 2001). Although CD45 was identified to be a critical SC35 target in T cell signaling, it is unlikely to be the only target underlying the developmental block, which appeared more dramatic than that observed in CD45 null mice. The difficulty in gene-targeting studies of SR proteins is the lack of an experimental system to conduct functional studies without complications caused by defects in cell proliferation or associated with cell death. Despite the fundamental requirement for essential splicing factors in cell physiology and animal development, their potential contribution to disease should not be underestimated, since recent linkage studies identified mutations in three separate essential splicing factors in retinitis pigmentosa, a dominant eye degeneration disease (Faustino and Cooper, 2003). No disease, however, has been directly linked to mutations in SR proteins.

Given the likely linkage of splicing enhancer mutations to human diseases and the strategic role of SR proteins in recognition of splicing enhancers, we have taken advantage of conditional SR protein knockout mice generated to investigate their functions in organ physiology. Here we report a striking phenotype associated with SC35 ablation in the heart. The cardiac system was chosen because adult heart is largely composed of nondividing cardiomyocytes, which may allow functional dissection of SR proteins in the absence of compound effects on cell proliferation. Strikingly, SC35 ablation during early cardiogenesis had no detectable effect on heart development and did not cause massive cell death. However, heart function was clearly compromised as SC35-deficient hearts developed dramatic cardiac hypertrophy and chamber dilation in the adult. Detailed molecular analysis showed that SC35 ablation in cardiomyocytes caused downregulation of the cardiac-specific ryanodine receptor 2 (RyR2) in the absence of a general effect on global gene expression and that such downregulation led to a specific excitation–contraction (EC) defect revealed by functional studies on isolated cardiomyocytes. The involvement of SC35 in heart disease uncovered in this study is consistent with a recent finding that linked SC35 expression to heart failure in humans (Hein *et al*, 2003). Thus, our studies have not only defined a general model to address the function of SR proteins *in vivo* but also illustrated a new potential pathway for heart disease in humans.

Results

Germline and tissue-specific ablation of SC35 result in distinct phenotypes

We previously described the conditional SC35 knockout mouse in which the SC35 gene was bracketed by LoxP sites (Wang *et al*, 2001). Conversion of the conditional allele to germline or tissue-specific knockout was accomplished by using the strategies illustrated in Figure 1. The ZP3-Cre transgenic mouse expresses the Cre recombinase in unfertilized oocytes (Lewandoski *et al*, 1997). Upon breeding with the floxed SC35 mouse, the gene was deleted in oocytes of F1 animals to produce heterozygous germline knockouts, which

could be further crossed to examine the role of SC35 in embryonic development (Figure 1B). To ablate SC35 in the heart, we crossed the floxed SC35 mouse with a Cre knockin mouse in which the Cre recombinase was placed under the promoter of the myosin light chain 2v (MLC-2v) to drive Cre expression specifically in ventricle cardiomyocytes at the onset of cardiogenesis (E8.5) (Chen *et al*, 1998). In Cre-positive and homozygous floxed SC35 mice (determined by genotyping tail DNA), the SC35 gene is targeted in the heart, but remains intact in other tissues (Figure 1C).
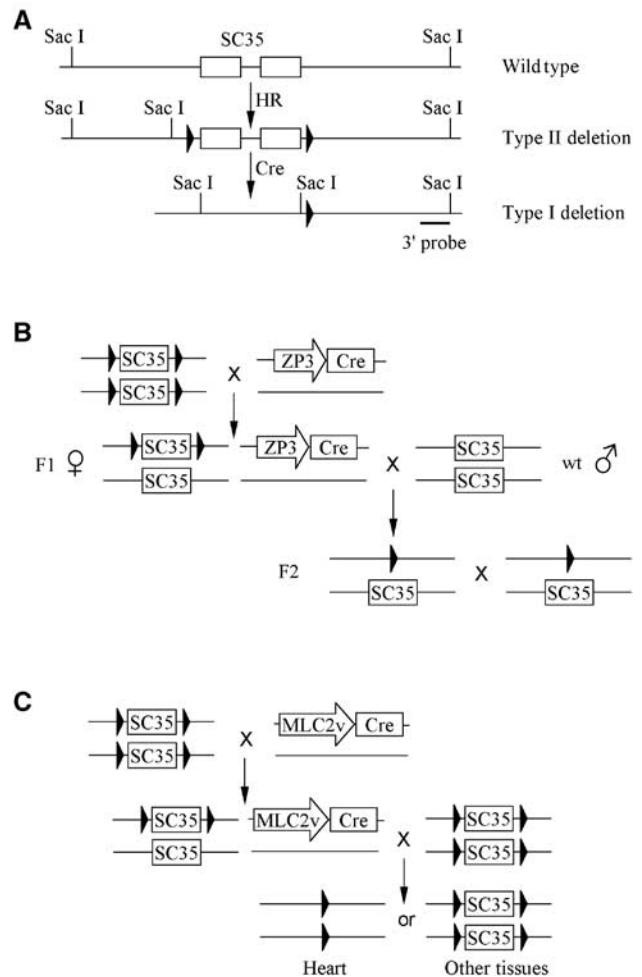

Figure 1 Germline and ventricle-specific deletion of SC35. (**A**) Map of the floxed SC35 locus generated by homologous recombination (HR) and Cre-mediated conversion. Generation of floxed SC35 mouse (type II deletion) was as previously described (Wang *et al*, 2001). Key *SacI* sites are illustrated and the 3′ probe was used to discriminate among wild type, type II and type I deletions. (**B**) Strategy to generate SC35 knockout in the germline. The zona pellucida 3 (ZP3) gene is expressed exclusively in the primary oocyte prior to the completion of the first meiotic division. After crossing floxed homozygous SC35 mice with ZP3-Cre transgenic mouse, the F1 female floxed SC35/Cre⁺ progeny were then mated with wild-type male mice to generate heterozygous SC35 type I deletions in the germline. Heterozygous SC35 knockout mice were mated with each other to produce homozygous knockout animals. (**C**) Strategy to generate ventricle-specific SC35 knockout. The MLC-2v promoter is turned on to express Cre at E8.5. After crossing floxed homozygous SC35 mice with the MLC2v-Cre knockin mouse, the double heterozygous floxed SC35/Cre⁺ mice were then crossed with homozygous floxed SC35 mice. This cross should generate 25% Cre⁺ mice in which SC35 was specifically ablated in the heart.

Breeding of germline-deleted SC35 heterozygous mice resulted in no homozygous animals at birth. We analyzed mice at several embryonic stages and found no homozygous mice dating back to E7.5 (Table 1). These results clearly show that deletion of the SC35 gene caused early embryonic lethality, a phenotype similar to that reported for SRp20 (Jumaa *et al*, 1999). Surprisingly, tissue-specific ablation of SC35 in heart ventricles had no effect on animal viability as homozygous animals were recovered at the normal Mendelian frequency (Table 2). Southern blotting analysis demonstrated ventricle-restricted deletion of the SC35 gene (Figure 2A). Note that deletion of the gene appeared incomplete in both the left and right ventricles because cardiomyocytes only contribute to 14% of the total cell number in ventricles and 90–95% are binucleated; thus, only ∼24% of the DNA content of ventricular tissue is from the cardiomyocyte population (Soonpaa *et al*, 1996). The observed level of deletion agrees with other reports using the MLC-2v-Cre line, which indicates >80% targeting efficiency in cardiomyocytes (Chen *et al*, 1998). Because cardiomyocytes occupy ∼80% of the cell volume in the heart and thus contribute to the bulk amount of total transcribed RNA, we were able to confirm by quantitative PCR a marked reduction (∼70%) of the SC35 transcript in the heart (Figure 2B). We could not directly verify the reduction of the corresponding protein because SC35 and most other SR proteins are not detectable in the heart by Western blotting with existing antibodies (Hanamura *et al*, 1998). The low level of SC35 in the heart implies that either the function of the protein is not required or is a rate-limiting factor for a narrow set of targets in the heart. The latter possibility is consistent with the analysis described below.

Finally, we have followed SC35-deficient mice for more than 1 year. Interestingly, the mutant mice had a normal life span, which is in contrast to similarly constructed SF2/ASF mutant mice, all of which died around 7 weeks after birth (Figure 2C). Characterization of SF2/ASF ablation in the heart will be described separately. Together, the results clearly

document the nonlethal phenotype associated with SC35 ablation in cardiomyocytes and illustrate distinct functions for distinct SR proteins in the heart.

SC35 ablation did not impair cardiomyocyte proliferation in vivo

The Mendelian recovery of SC35 mutant mice from the cross with MLC-2v-Cre mice is surprising, given the early embryonic lethality associated with germline deletion of both SRp20 and SC35 and the requirement of SF2/ASF for cell viability in chicken DT40 cells, which together suggest an essential role of SR proteins for cell survival. The mutant mice, however, are not completely normal (see below). The heart is unique in that most cell proliferation takes place during embryonic development, and differentiated cardiomyocytes then switch to hypertrophic growth after birth (Pasumarthi and Field, 2002).

To evaluate the potential impact of SC35 ablation on cardiomyocyte proliferation, we determined the cell division index by BrdU labeling. We chose E18.5 embryos for analysis because this stage has passed the initial burst of cell division and differentiation of cardiomyocytes from E8.5 to E11.5, and thus potential residual effects of SC35 deletion would be minimal. At this stage, most proliferating cardiomyocytes are at the periphery of the developing heart, consistent with a previous study (Soonpaa *et al*, 1996), and BrdU incorporation was indistinguishable between mutants and littermate controls (Figure 3A). We also carried out a BrdU pulse–chase experiment to determine the number of cells withdrawing from cell division, which would allow the detection of smaller cell proliferation defects (proliferating cells will become BrdU negative and cells withdrawing from division will contain BrdU after chasing). Again, we saw no difference between wild-type and SC35 targeted mice, and in both cases little mitotic withdrawal was detected (data not shown). We also conducted the TUNEL assay and found no sign of apoptosis in both wild-type and SC35-deficient hearts (data not shown). We conclude that SC35 ablation had little impact on cardiomyocyte viability or cell proliferation in the developing heart.

SC35 mutant mice developed typical dilated cardiomyopathy

Although SC35 ablation had little effect on heart development and mortality, mutant mice started to display clear disease symptoms upon entering adulthood, including weakness in activity and pregnancy-induced mortality in females. To characterize the disease phenotype, we conducted time-course echocardiography to assess global cardiac function in SC35-deficient mice in comparison with age-matched littermate controls (Table 3). The data show that the mutant mice had a normal heart rate, and displayed little alteration in interventricular septum thickness (IVS) or left ventricular posterior wall thickness (PW). In contrast, both left ventricular end-diastolic dimensions (LVEDD) and end-systolic dimensions (LVESD) were markedly increased 5–6 weeks after birth. The percent fractional shortening (%FS) and mean velocity of circumferential fiber shortening (mean Vcf), indicators of systolic cardiac function, were severely reduced, indicating a severe contraction defect in the mutant heart. This phenotype coupled with further chamber dilation in the advanced stages (see below) demonstrates that SC35

Table 1 Early embryonic lethality resulting from germline deletion of SC35 (SC35(+/−) × SC35(+/−))

Embryonic age (dpc)		Genotype			Total
	Litter	+/+	+/−	−/−	
7.5	1	3	4	0	7
8.5	2	5	9	0	14
10.5	1	3	4	0	7
12.5	1	1	5	0	6
13.5	1	2	4	0	6
Pups at birth		45	92	0	137
Total		59	118	0	177

Table 2 Mendelian recovery of SC35 targeted mice in the heart

	SC35(+/II)/Cre(+/−) × SC35(II/II)/Cre(−/−)	
	Cre(−/−)	Cre(+/−)
SC35(+/II)	19	15
SC35(II/II)	14	19

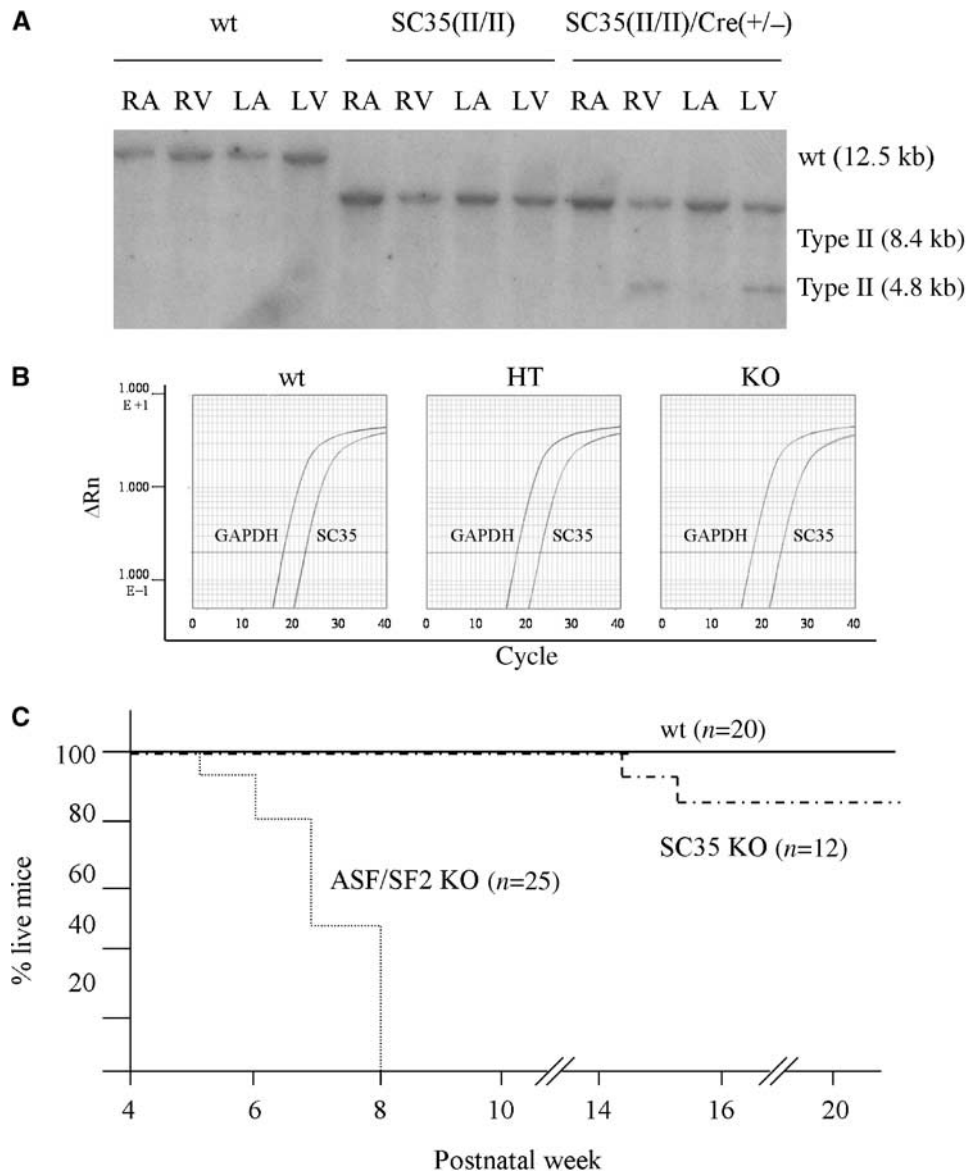Note: Floxed SC35 allele is here referred to as type II deletion.

Figure 2 Nonlethal phenotype with SC35 ablation in the heart. (**A**) Specificity and efficiency of MLC2v-Cre-mediated recombination in the heart. Genomic DNA from right atrium (RA), left atrium (LA), right ventricle (RV) and left ventricle (LV) were digested with *SacI* and analyzed by Southern blotting. Recombination is restricted to the ventricles. (**B**) Quantitative PCR analysis of the SC35 transcript. The GAPDH transcript was analyzed as a control. (**C**) Mortality curve for SC35 ablation in the heart. Over 80% SC35-deficient mice have a normal life span similar to their littermates in the same cage. In contrast, all similarly targeted SF2/ASF mice died within 8 weeks after birth.

ablation in the heart caused a disease state similar to a human heart disease condition known as dilated cardiomyopathy (DCM) (Chien, 2000).

Interestingly, the cardiac malfunction was not evident in young mice at 3 weeks of age, and the disease phenotype developed during the juvenile-to-adult transition, indicating that the functional defect may have become manifest due to the gradual increase of workload on the heart. To further characterize the disease phenotype, we conducted a series of morphological analysis. Consistent with the echocardiography data, the mutant heart appeared normal initially and became enlarged 5 weeks after birth (Figure 3Ba–d), which is coincident with the disease phenotype detected by echocardiography. Histological analysis revealed that cardiomyocytes

in the mutant heart appeared normal 3 weeks after birth, but subsequently showed compensatory cardiac hypertrophy (Figure 3Be–h). Because cardiac hypertrophy reflects a specific type (pathological) of cell growth, this observation coupled with normal heart development shows that SC35 is not required for both physiological and pathological cell growth in the cardiomyocyte lineage. Although the mutant animals have a normal life span, extensive fibrosis and myofibril disarray were evident by trichrome staining (Figure 3Ca–b), and the mutant hearts were dramatically enlarged with severe chamber dilation (Figure 3Ce–f) in advanced stages. However, the basic contractile apparatus (the sarcomere structure) remained unaltered by electron microscopy even after the disease was fully developed

(Figure 3Cc–d). Together, these results establish the late onset of the disease phenotype and demonstrate the functional requirement of SC35 for normal heart performance.

SC35 ablation downregulated RyR2 but had little impact on global gene expression

The nonlethal disease phenotype resulting from SC35 ablation provides a model system to explore potential splicing defects *in vivo*. We thus decided to conduct gene expression
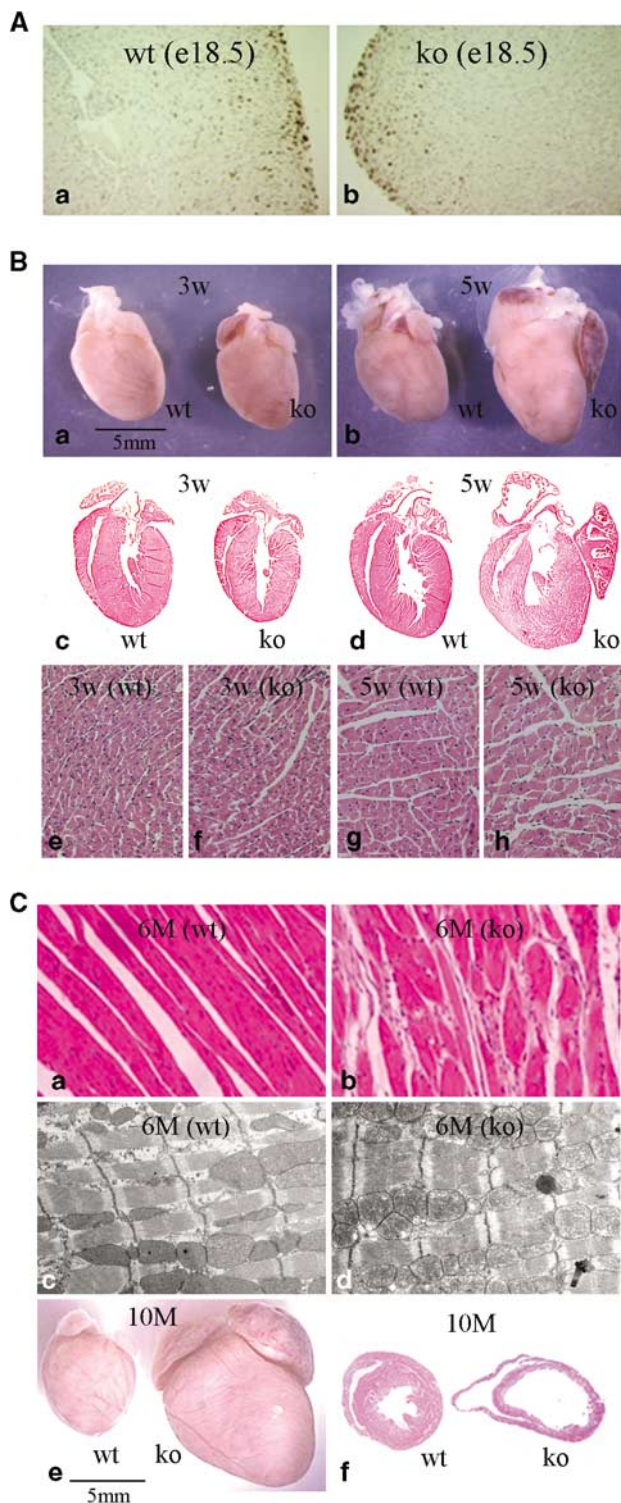
profiling experiments using Affymetrix microarrays based on the following rationales. First, it represented an opportunity to test the global effect of a presumed essential splicing factor on gene expression. Use of the profiling approach to detect potential splicing defects is based on the possibility that a mis-spliced RNA may be quickly decayed in the cell, although other indirect effects, for example, resulting from downregulation of some transcription factors are also possible. As recently illustrated in a myotonic dystrophy model, an acquired splicing defect due to CTG expansion led to downregulation of a muscle-specific chloride channel mRNA, which was triggered by the inclusion of premature stop codons in retained introns (Charlet *et al*, 2002; Mankodi *et al*, 2002). The downregulation likely follows the so-called nonsense mediated decay (NMD) pathway (Maquat and Carmichael, 2001). Furthermore, through analysis of specific molecular changes, it might be possible to obtain first approximation of the mechanism underlying the disease phenotype.

To conduct microarray analysis, we chose to compare SC35-deficient hearts and littermate controls at the beginning of disease onset (4 weeks after birth). Three hearts in each category were isolated and total RNA was extracted from dissected ventricles. Total RNA samples were then subjected to microarray analysis on Affymetrix mouse U74Av2 chips containing ~ 8000 known genes in the mouse genome. A large number of genes were upregulated (Figure 4). Close inspection of these upregulated genes indicates that many of them are markers for cardiac hypertrophy (such as natriuretic peptide precursor also known as atrial natriuretic factor or ANF, skeletal actin, etc.); others are markers for fibrosis (such as procollagens). Northern blotting analysis confirmed a dramatic induction of ANF and a modest elevation of skeletal actin in disease hearts, whereas other critical cardiac-specific transcripts such as components of the troponin T complex and the striated muscle-specific LIM domain protein MLP were unaltered (Figure 5A). These results show that the microarray analysis accurately reported molecular changes generally associated with the heart disease phenotype.

Because most upregulation events likely reflect the progression of cardiac hypertrophy, rather than causative changes in expression, we focused on downregulated genes. Surprisingly, little downregulation was observed, indicating a lack of global NMD or other indirect effects triggered by SC35

Figure 3 Histological and pathological analysis of SC35-deficient hearts. (**A**) Cell proliferation assay by BrdU labeling. Mice were injected with BrdU at E18.5 and ventricles were isolated 22 h later. Paraffin sections of ventricles were blotted with biotinylated anti-BrdU antibody followed by staining with HRP-conjugated streptavidin in the presence of the substrate AEC. Proliferating cells were stained as brown dots in the periphery of the heart. (**B**) Isolated mutant hearts and their littermate controls at 3 and 5 weeks after birth (a and b); H&E-stained coronal sections showing normal cardiac histology 3 weeks after birth, but chamber enlargement and cardiomyocyte hypertrophy at postnatal 5 weeks (c–h). (**C**) Extensive fibrosis and myofibril disarray in SC35-deficient hearts were evident at an advanced stage (a and b). However, the sarcomere structure appeared normal under the electron microscope (c and d). Dramatic heart enlargement and chamber dilation were seen with the SC35 knockout hearts at late stages (c and d). The stages (in months) indicate the time when the hearts were collected for analysis, which do not represent the phenotype onset points.

Table 3 Time-course analysis of *in vivo* cardiac size and function by echocardiography

	Heart rate (beats/min)	IVS (mm)	PW (mm)	LVEDD (mm)	LVESD (mm)	%FS	Vcf (circ/s)
Wild type							
Week 3 ($n=4$)	430 ± 47	0.51 ± 0.04	0.51 ± 0.06	2.64 ± 0.52	1.17 ± 0.37	56.4 ± 6.5	9.8 ± 1.66
Week 4 ($n=3$)	488 ± 11	0.56 ± 0.03	0.6 ± 0.05	3.32 ± 0.31	1.66 ± 0.26	50.4 ± 3.5	8.36 ± 0.3
Week 5 ($n=3$)	501 ± 11.53	0.62 ± 0.03	0.63 ± 0.07	3.4 ± 0.08	1.58 ± 0.1	53.6 ± 1.95	9.47 ± 0.64
Week 6 ($n=3$)	365 ± 60.13	0.58 ± 0.03	0.57 ± 0.03	3.54 ± 0.06	1.96 ± 0.26	44.68 ± 6.64	7.48 ± 2.41
Week 9 ($n=4$)	426 ± 77.1	0.6 ± 0.02	0.65 ± 0.04	3.67 ± 0.22	2.19 ± 0.5	40.86 ± 11.11	8.29 ± 3.66
Knockout							
Week 3 ($n=4$)	446 ± 58	0.53 ± 0.04	0.56 ± 0.06	2.72 ± 0.82	1.36 ± 0.47	50.4 ± 5.5	8.47 ± 1.63
Week 4 ($n=3$)	420 ± 54	0.53 ± 0.02	$0.52 \pm 0.02*$	3.53 ± 0.36	2.18 ± 0.29	$38.3 \pm 2.7**$	$5.83 \pm 0.76**$
Week 5 ($n=3$)	506 ± 8.72	0.58 ± 0.04	0.55 ± 0.04	4.16 ± 0.54	$3.22 \pm 0.4***$	$22.39 \pm 0.61***$	$3.81 \pm 0.33***$
Week 6 ($n=3$)	410 ± 19.01	0.55 ± 0.06	0.52 ± 0.09	$4.29 \pm 0.26**$	$3.47 \pm 0.51**$	$19.41 \pm 6.98**$	3.64 ± 1.63
Week 9 ($n=2$)	444 ± 48.08	0.56 ± 0	0.58 ± 0.06	$4.64 \pm 0.32**$	$3.63 \pm 0.34*$	21.75 ± 1.95	4.78 ± 0.21

IVS: interventricular septum thickness; LVEDD: end-diastolic LV dimensions; LVESD: end-systolic LV dimensions; PW: LV posterior wall thickness; %FS: fractional shortening; Vcf: velocity of circumferential fiber shortening.
Statistical significance (wild type versus ko): $*P < 0.05$, $**P < 0.01$, $***P < 0.001$.

ablation. A similar observation was also made with SF2/ASF in chicken DT40 cells (Lemaire *et al*, 2002). Such a lack of global effect on gene expression may be partly due to functional redundancy among SR proteins as shown in the fly (Hoffman and Lis, 2000). Interestingly, one of the few downregulated transcripts detected is the cardiac-specific RyR2, which functions as a crucial Ca^{2+}-releasing channel in SR that initiates muscle contraction (Chien, 2000). Thus, SC35 may be essential for efficient processing of this huge transcript consisting of more than 100 exons (Nakai *et al*, 1990).

Because of the vital role of RyR2 in heart function, its downregulation would explain the disease phenotype. However, it is important to keep in mind that the downregulation may result directly from SC35 inactivation, or indirectly as a consequence of the disease phenotype triggered by other molecular defects, since RyR2 is generally downregulated in failing hearts (Marx and Marks, 2002). To determine if RyR2 downregulation in the SC35-deficient heart preceded the disease phenotype, we analyzed the level of the RyR2 transcript by quantitative PCR, and found a 2.5-fold reduction in comparison to GAPDH in the mutant hearts at both perinatal and postnatal stages (Figure 5B). Western blotting analysis of RyR2 in enriched SR fractions showed a similar reduction at the protein level in comparison with the constant SR marker calsequestrin (Figure 5C). Additional Western blotting analysis indicated that other key Ca^{2+} regulatory factors including SERCA2 and Phospholamban remained unaltered (data not shown). Together, these data indicate that RyR2 may require SC35 for its efficient processing and therefore expression, and the processing defect may directly contribute to the disease phenotype. Further attempts to localize specific splicing defects in RyR2 by RT–PCR failed to reveal aberrant RyR2 isoforms, but it remains possible that defective RyR2 mRNAs (such as those with retained introns) escaped detection because they may represent unstable minor species in SC35-deficient hearts.

SC35-deficient heart exhibited frequency-dependent EC defects

In order to obtain functional evidence that can be directly attributed to RyR2 downregulation, we conducted a series of electrophysiological experiments to characterize the functional defect triggered by SC35 ablation in the heart. Single

cardiomyocytes were isolated from wild-type and SC35-deficient hearts at the age of postnatal 3 weeks when the disease phenotype was yet to become evident. Under a confocal microscope, freshly isolated cardiomyocytes were loaded with the Ca^{2+} indicator fluo-4 to monitor Ca^{2+} transients and cell contraction in response to electrical pacing at different frequencies. No significant change of resting intracellular Ca^{2+} and diastolic Ca^{2+} was detected at each frequency tested (Figure 6A and B). Furthermore, no difference in Ca^{2+} transients and contraction was observed at 0.5 Hz stimulation (Figure 6A and B, left panels). These results show that the mutant cardiomyocytes are functionally normal under unstressed conditions, which agrees with the general functionality of the SC35-deficient heart at the organ and animal levels.

When the pacing frequency was elevated, however, we detected a significant decrease in both Ca^{2+} transients and cell contraction (Figure 6A and B, right panels). Statistical analysis documented these frequency-dependent EC coupling defects (Figure 6C and D). These observations indicate that the functional defect in SC35-deficient hearts is latent and only becomes detectable with increasing workload, which explains the stress-induced death of otherwise phenotypically normal mice (Figure 2C). Most importantly, the frequency-dependent reduction of Ca^{2+} transients concurs fully with the functional defect expected from a reduced RyR2 density on the sarcoplasmic reticulum. Interestingly, we also observed faster relaxation kinetics of Ca^{2+} transients at all stimulation frequencies tested (Figure 6B), suggesting either an enhanced Ca^{2+} re-uptake or a reduced release in the descending phase of the Ca^{2+} transient, which may also relate to RyR2 downregulation. This defect compounded with reduced Ca^{2+} transients would significantly weaken the EC coupling in response to increasing workload, thereby triggering a compensatory pathway in the form of cardiac hypertrophy as observed during the juvenile-to-adult transition.

Discussion

The present study explored the heart as an experimental system to study splicing regulation *in vivo*. This system offers distinct advantages over other cell and animal models as cell proliferation and functional output can be investigated at

Up- and down-regulated genes in SC35 deficient heart

PEAK FOLD	ACC #	DESCRIPTION
7.27	D13664	Osteoblast specific factor 2 (fasciclin I-like)
6.89	K02781	Natriuretic peptide precursor type A
5.70	X13986	Secreted phosphoprotein 1
5.27	X51547	Plysozyme structural
4.95	M21050	Lysozyme
4.71	M70642	Connective tissue growth factor
4.21	AJ223208	Cathepsin S
3.89	AW121179	Microfibrillar associated protein 5
3.89	X66976	Procollagen, type VIII, alpha 1
3.84	U03419	Procollagen, type I, alpha 1
3.79	M12347	Actin, alpha 1, skeletal muscle
3.67	AF041847	Ankyrin-like repeat protein
3.62	X60367	Retinol binding protein 1, cellular
3.47	D16497	Natriuretic peptide precursor type B
3.31	X58251	Procollagen, type I, alpha 2
3.25	X53928	Biglycan
3.19	X66449	S100 calcium binding protein A6 (calcyclin)
2.96	D00613	Matrix gamma-carboxyglutamate (gla) protein
2.83	AV234303	Procollagen, type III, alpha 1
2.83	L29454	Fibrillin 1
2.82	X52046	Procollagen, type III, alpha 1
2.77	K02782	Complement component 3
2.67	AW122012	RIKEN cDNA 2610001E17 gene
2.57	M69260	Annexin A1
2.57	AF024637	TYRO protein tyrosine kinase binding protein
2.56	AF036164	Serine (or cysteine) proteinase inhibitor, clade F member 1
2.54	M22531	Complement component 1, q subcomponent, beta polypeptide
2.51	M91380	Follistatin-like
2.48	M29009	Complement factor H-related protein
2.42	X75285	Fibulin 2
2.41	D00466	Apolipoprotein E
2.41	M12660	Complement component factor h
2.28	X98471	Epithelial membrane protein 1
2.23	D45889	Chondroitin sulfate proteoglycan 2
2.22	U13705	Glutathione peroxidase 3
2.21	AF057156	Small proline-rich protein 1A
2.15	AA919594	Elastin
2.14	U49513	Small inducible cytokine A9
2.14	AV003419	Annexin A1
2.11	U41739	Four and a half LIM domains 1
2.07	X58861	Complement component 1, q subcomponent, alpha polypeptide
2.05	X15986	Lectin, galactose binding, soluble 1
2.03	V00755	Tissue inhibitor of metalloproteinase
2.03	AF013262	Lumican
2.02	M74570	Aldehyde dehydrogenase family 1, subfamily A1
−2.03	Z49204	Nicotinamide nucleotide transhydrogenase
−2.06	AW226939	Carboxylesterase 3
−2.06	AI850363	Muscle glycogen phosphorylase
−2.11	X78667	Ryanodine receptor 2, cardiac
−2.11	D86037	ATP-binding cassette, sub-family C (CFTR/MRP), member 9
−2.22	AW226939	Carboxylesterase 3

−6.25 ▉▉▉▊ ▊▉▉▉ 6.25

Figure 4 Profiling gene expression in SC35-ablated ventricles. Total RNA was extracted from SC35-deficient ventricles and littermate controls, converted to cRNA, and hybridized to Affymetrix U74Av2 chips. Results are from three independent experiments for both wild-type and mutant mice. Fold changes (also highlighted by gray degree), gene ID, and names are listed.

different developmental stages. Because most differentiated cardiomyocytes do not divide in adulthood, the heart system allows studies of functional defects without complications associated with general requirements for cell proliferation. This system is generally applicable to other splicing factors and regulators. In fact, the heart has been a favorable model to study gene expression and splicing regulation. One of the most striking aspects of the heart is developmental reprogramming of gene expression at both the transcriptional and splicing levels during the postnatal period in response to increasing workload. For instance, the expression of the slow

skeletal troponin I (ssTnI) in developing heart is gradually replaced after birth by the cardiac-specific troponin I (cTnI) (Schianffino *et al*, 1993), and such a transition is critical for heart performance in the adult (Huang *et al*, 1999). Furthermore, many heart specific transcripts undergo developmental and tissue-specific regulation of alternative splicing (Hodges and Bernstein, 1994). For example, the cardiac troponin T gene expresses multiple isoforms in the embryo, but only one isoform in the adult (Townsend *et al*, 1995). A recent functional study showed that such an isoform switch correlates with changes in Ca^{2+} sensitivity of the troponin
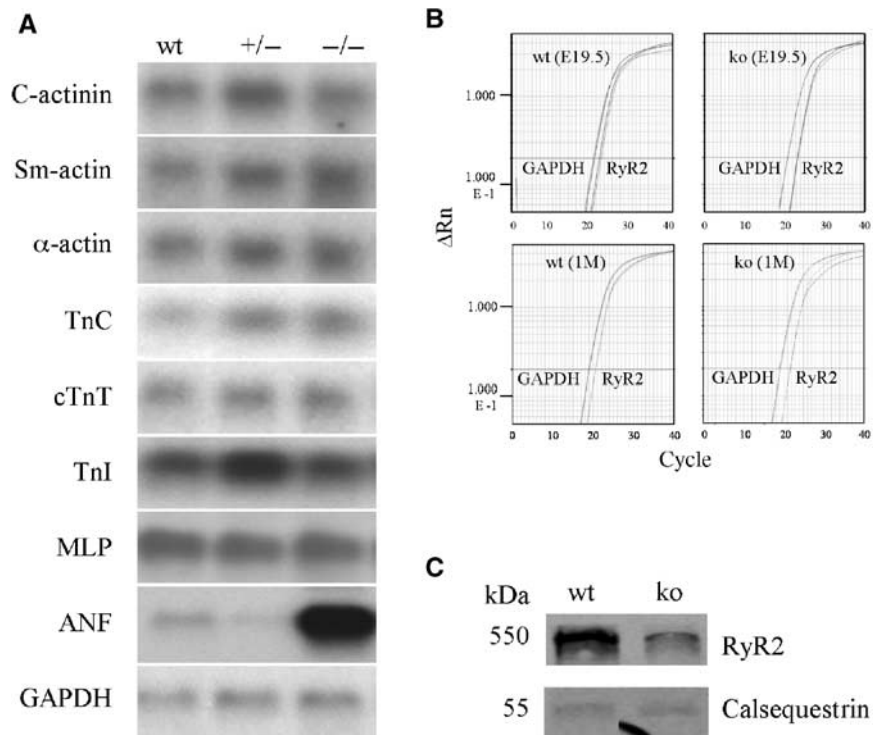
Figure 5 Molecular characterization of SC35-deficient hearts. (**A**) Northern blotting analysis of both hypertrophy markers and critical components of the troponin complex in wild-type, hetero-, and homozygous SC35-ablated mice. Note that an apparent elevation of TnI expression in a heterozygous heart was not a reproducible result. (**B**) Quantitative PCR analysis of RyR2 RNA at two different developmental stages (E19.5 and postnatal 1 month). GAPDH was analyzed as a control. Each experiment was duplicated. (**C**) Western blotting analysis of RyR2 protein in an sarcoplasmic reticulum-enriched cellular fraction. The sarcoplasmic reticulum resident marker calsequestrin was analyzed as a loading control.

complex during development (Gomes *et al*, 2002). Numerous reports have documented the causal effect of point mutations in an array of cytoskeletal proteins in human heart disease, but it remains unclear whether any of these mutations cause disease by disrupting splicing regulation. The current study highlights the functional consequence of conditional ablation of a *trans*-acting splicing factor in the mouse model.

SR splicing factors have been extensively studied. Genetic inactivation experiments indicate that all SR proteins tested so far are critical for early embryonic development and cell survival (Wang *et al*, 1996). In this regard, the observed diseased, but nonlethal, phenotype resulting from SC35 ablation in the heart is surprising, and suggests that the requirement for cell viability may be both SR protein-dependent and cell type-dependent. Consistently, we also observed a late onset phenotype with SF2/ASF ablation in the heart (Figure 2C). Thus, at least two SR proteins tested are not essential for cell viability in the cardiac cell lineage.

Although SC35 is not required for cell viability in the heart, it is clearly important for heart function. Interestingly, the disease phenotype appeared about 5 weeks after birth. Two possibilities may explain the timing of disease onset. SC35 may be critical for processing of a defined set of targets during postnatal reprogramming of gene expression. Alternatively, SC35-deficient cells are not normal, but the functional defect becomes detectable only in the adult in response to increasing workload. Our observation of RyR2 downregulation and the associated frequency-dependent EC coupling defects support the second possibility.

Although RyR2 downregulation appeared to be sufficient to explain the disease phenotype, we also considered other

potential subtle changes in alternative splicing that may additionally contribute to the disease phenotype, such as induction of cardiac hypertrophy. For example, the histone deacetylase-9 (HDAC9) plays a general role in repressing hypertrophic programming (Zhang *et al*, 2002). HDAC9 is targeted to the nucleus via a nuclear localization signal in exon 7, which is subject to alternative splicing (Zhou *et al*, 2001). It is thus conceivable that a splicing defect causing exon 7 skipping would induce derepression of a range of hypertrophy markers in the SC35-deficient heart. We tested this possibility by RT–PCR and found no change in HDAC9 splicing. A number of other candidates tested, but without apparent change, include cTnT whose splicing is regulated during development and aberrant splicing has been linked to DCM (Biesiadecki *et al*, 2002), the *PDZ-LIM* domain protein called Cypher whose cardiac and skeletal muscle-specific isoforms are each essential for mouse viability (Huang *et al*, 2003), the focal adhesion kinase (FAK) whose alternative splicing can induce autophosphorylation of the kinase (Toutant *et al*, 2002), leading to cytoskeletal disorganization during cardiac hypertrophy (Kovacic-Milivojevic *et al*, 2001), and Ca^{2+}/calmodulin kinase IIδ which expresses tissue-specific isoforms to regulate Ca^{2+} handling and EC coupling in the heart (Zhang *et al*, 2003). Although numerous other candidates implicated in heart disease remain to be assayed, these results imply that SC35 has a limited set of targets in the heart, most likely due to functional redundancy with other SR proteins.

Our current conclusion that SC35 plays a critical role in heart disease is derived from a reverse genetic approach in a model system. Since SC35 is required for early embryonic
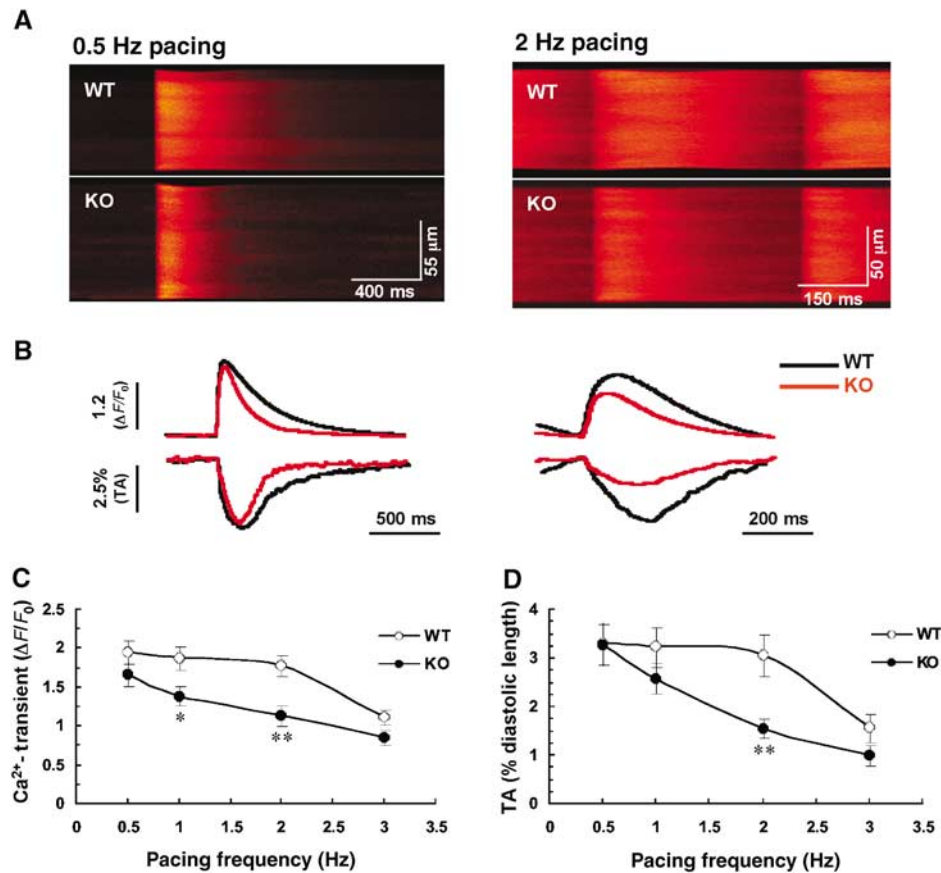
Figure 6 Deficient EC coupling in SC35 knockout cardiomyocytes. (**A**) Typical confocal Ca^{2+} images of single isolated cardiomyocytes from wild-type or knockout mice. Cultured cells were loaded with fluo-4 followed by pacing at designated frequencies. Line-scan images are displayed with time and space on the abscissa and ordinate, respectively. (**B**) Traces of spatially averaged Ca^{2+} transients (top) and the corresponding cell shortenings (bottom, downward defections). (**C**) Frequency dependence of peak Ca^{2+} transient ($\Delta F/F_0$, where F_0 refers to the fluo-4 signal at rest). (**D**) Frequency dependence of twitch amplitude (TA, presented as percent diastolic cell length). $*P<0.05$; $**P<0.01$ by Student's *t*-test. $N=17-22$ for each data point.

development, embryos with lethal mutations in such an essential gene would be selected against before reaching adulthood to cause heart disease. However, several scenarios make our finding relevant to naturally occurring heart disease in humans. First, many essential genes may carry mutations that cause partial loss of function and certain tissues may be particularly sensitive to such mutations, examples of which were recently documented with several essential splicing factors in retinitis pigmentosa (Faustino and Cooper, 2003).

Heart disease may also be triggered by mutations in *cis*-acting SC35 responsive elements in disease-causing transcripts. Forward genetics has identified a dozen inheritable heart disease genes, most of which are components of the contractile apparatus in the heart (Bonne *et al*, 1998; Towbin, 1998). In addition, many gene products including transcriptional factors, signaling molecules, and Ca^{2+} regulators have been linked to various forms of cardiac disease (Chien, 2000). Point mutations either inherited or acquired in those genes may disrupt exonic splicing enhancers recognized by SC35 or other RNA-binding proteins, thereby causing aberrant splicing and leading to a disease phenotype. One way to compensate for a splicing defect is to elevate the level of a specific *trans*-acting factor. Consistent with this possibility, it was recently reported that SC35 expression was induced in failing heart in humans, indicating that SC35 may indeed be part of

the response pathway to defend against cardiac defects (Hein *et al*, 2003).

Another disease mechanism may be due to partial loss of SC35 function as a result of viral infection, which has long been known to cause myocarditis and DCM (Vercellotti, 2001; Mason, 2002). In addition to autoimmune responses, which may cause general myocardial damages, viral infection also alters gene expression in infected cells. Strikingly, SR protein function and regulation have been shown to be cellular targets for three different viruses. Adenoviral infection was found to induce massive reorganization of the cellular splicing machinery (Jimenez-Garcia and Spector, 1993; Bridge *et al*, 1995). It was later shown that the virus E4-ORF4 protein interacts with the cellular phosphatase 2A as well as a subset of SR proteins, thereby inducing SR protein dephosphorylation (Kanopka *et al*, 1998; Estmer Nilsson *et al*, 2001). Since phosphorylation is known to regulate the localization of SR proteins (Gui *et al*, 1994; Misteli and Spector, 1998) and their functions in spliceosome assembly (Mermoud *et al*, 1994), SR proteins were functionally inactivated in the infected cells (Kanopka *et al*, 1998). Induction of SR protein dephosphorylation and inhibition of splicing were also shown in vaccinia virus-infected cells, and the effects were mediated by the virus-encoded protein phosphatase VH1 (Huang *et al*, 2002). Lastly, splicing inhibition in herpes

simplex virus-infected cells was recently revealed to be due to the specific virus protein ICP27 (Lindberg and Kreivi, 2002). In this case, ICP27 induces SR protein dephosphorylation and reorganization of the splicing machinery via a specific interaction with SR protein-specific kinases (Sciabica *et al*, 2003). Together, these findings strongly suggest that SR protein function and regulation are frequent targets during viral infection. Because our current findings demonstrate an unequivocal role of a prototypical SR protein in heart function, we here propose a new disease paradigm where viral infection causes myocarditis by inducing partial loss of function of critical *trans*-acting splicing factors, such as SR proteins and their regulators.

Methods

Generation of SC35 knockout mice
Floxed SC35 mice were previously described (Wang *et al*, 2001). Germline deletion was accomplished by crossing homozygous floxed SC35 mice with the ZP3-Cre transgenic mouse (Lewandoski *et al*, 1997). F1 Cre-positive mice were identified by dot blotting using a Cre-specific probe. The female mice were crossed with wild-type mice to produce heterozygous germline SC35 knockout mice, which were then crossed with each other to obtain SC35 null mice. To target SC35 in ventricular cardiomyocytes, homozygous floxed SC35 mice were crossed with the MCL2v-Cre-knockin mouse (Chen *et al*, 1998). Cre-positive mice were crossed with homozygous floxed SC35 mice to obtain mice that were both Cre-positive and homozygous for floxed SC35. SC35 ablation in the heart was confirmed by dissecting heart tissues followed by Southern blotting analysis of *Sac*I-digested DNA.

Morphological and echocardiographic analysis
Hearts were dissected, washed in PBS containing 100 mM KCl, fixed in 10% neutrally buffered formalin overnight, paraffin-embedded and sectioned. Paraffin sections were stained with hematoxylin and eosin (H&E) or trichrome. To determine the cell proliferation state, BrdU was injected intraperitoneally in pregnant mice at 50 μg/g body weight. Paraffin sections were overlaid with biotinylated anti-BrdU antibody (Zymed), HRP streptavidin and substrate AEC (Vector Labs). For ultrastructural analysis, dissected hearts were washed once in PBS containing 100 mM KCl and then fixed by perfusion overnight in 4% paraformaldehyde and 2% glutaraldehyde at 4°C, and stained by the conventional osmium–uranium–lead method (Martone *et al*, 1999). For echocardiographic analysis, mice were anesthetized with Avertin (2.5%, 10 μl/g body weight). Littermates were used in all echocardiographic recordings.

Affymetrix microarray studies
Syntheses of cRNA and array hybridization were according to the Affymetrix protocol. In all, 10 μg of total Trizol-extracted RNA was converted to cDNA with the T7T24 primer and Superscript II RT. The cDNA was then used as template to synthesize second-strand cDNA with *Escherichia coli* DNA Pol I. Double-stranded cDNA was purified by phenol extraction and salt precipitation. In all, 5 μg of cDNA was used for the synthesis of biotin-labeled cRNA, purified with RNeasy column (Qiagen), and 50 μg was used for hybridiza-

tion on U74Av2 (Affymetrix) in the UCSD Cancer Center microarray core facility. Data analysis was according to Sasik *et al* (2002).

Western blotting of RyR2
Ventricle sarcoplasmic reticulum was prepared as described (Lokuta *et al*, 1997). Briefly, ventricles from 1-month-old mice were dissected and washed in PBS/100 mM KCl, cut into small pieces, and suspended in 1 ml of 154 mM NaCl/ 10 mM MOPS (pH 7.0) in the presence of proteinase inhibitors. Ventricle pieces were homogenized by polytron (PTMR 2100) for 2 min at 26 000 rpm and cell debris was removed in a microfuge at 4000 *g* for 20 min in the cold room. The supernatant was further cleared at 7000 *g* for 20 min. Sarcoplasmic reticulum microsomes in the supernatant were pelleted at 40 000 *g* in a Beckman SW55T1 rotor for 30 min at 4°C. The sarcoplasmic reticulum pellet was suspended in SDS sample buffer. In all, 40 μg of total protein was loaded on 4–20% gradient SDS–PAGE (Bio-Rad), blotted to nitrocellulose membrane, and probed with anti-RyR2 (Affinity BioReagents, cat# MA3-916) and anti-calsequestrin antibodies (BD Transduction Labs, cat# 611652).

Northern blotting
Northern blotting assay was performed as previously described (Wang *et al*, 2001). In all, 5–20 μg of total RNA extracted from ventricles was loaded per lane, blotted to Hybond nylon membrane (Amersham), and probed with end-labeled oligonucleotide (60–70 nt) corresponding to a specific sequence in the coding region of individual transcripts.

RT–PCR and Q-PCR
In all, 2 μg of total RNA was converted to cDNA in a 20 μl reaction with Superscript II RT (Invitrogen). In all, 1 μl of cDNA was used as template for PCR amplification (94°C for 30 s, 58°C for 30 s, and 72°C for 30 s). Real-time PCR was performed on the ABI Prism 7900 Sequence Detection System. Primer pairs designed to detect specific transcripts are as follows: SC35-F: 5′-GAG TCA TTC TGC TGA CAG C-3′; SC35-R: 5′-ATC ATC AGC TAG ATG TGC TC-3′; GAPDH-F: 5′-TAC ATG TTC CAG TAT GAC TC-3′; GAPDH-R: 5′-CCA CGA CAT ACT CAG CAC-3′; RyR2-89F: 5′-CGG CCT CAG TGA CCT CAT G-3′; RyR2-93R: 5′-TCA CTT TAG CAG TAT CGC TGG-3′.

Ca^{2+} transient and contraction measurement and statistical analysis
Single cardiomyocytes were isolated from the hearts of 2-week-old mice using a standard enzymatic procedure as described (Zhou *et al*, 2000). Isolated cardiomyocytes were loaded with the Ca^{2+} indicator fluo-4/AS (5 μmol/l for 15 min) (Molecular Probes) and field-stimulated at 0.5, 1, 2, or 3 Hz with perfusion solution containing 137 mM NaCl, 4.9 mM KCl, 1 mM CaCl$_2$, 1.2 mM MgSO$_4$, 1.2 mM NaH$_2$PO$_4$, 15 mM glucose, and 20 mM HEPES (pH 7.4). Confocal images were obtained using a Zeiss LSM 510 in the line-scan mode with the scanning line oriented along the long axis of cardiomyocytes, avoiding the nuclei. Image processing, data analysis, and presentation were performed using the IDL 5.5 software (Research System). Data were reported as mean±SEM. Student's *t*-test or ANOVA was applied on repeated measurements to determine the statistical signifi-

cance of a difference. A *P*-value of less than 0.05 was considered to be statistically significant.

Acknowledgements

References

Biesiadecki BJ, Elder BD, Yu ZB, Jin JP (2002) Cardiac troponin T variants produced by aberrant splicing of multiple exons in animals with high instances of dilated cardiomyopathy. *J Biol Chem* **277:** 50275–50285

Black DL (2000) Protein diversity from alternative splicing: a challenge for bioinformatics and post-genome biology. *Cell* **103:** 367–370

Bonne G, Carrier L, Richard P, Hainque B, Schwartz K (1998) Familial hypertrophic cardiomyopathy: from mutations to functional defects. *Circ Res* **83:** 580–593

Bridge E, Xia DX, Carmo-Fonseca M, Cardinali B, Lamond AI, Pettersson U (1995) Dynamic organization of splicing factors in adenovirus-infected cells. *J Virol* **69:** 281–290

Burge CB, Tuschl TH, Sharp PA (1999) Splicing of precursors to mRNA by the spliceosome. In *The RNA World II*, Gesteland RF, Cech TR, Atkins JF (eds), pp 525–560

Cartegni L, Chew SL, Krainer AR (2002) Listening to silence and understanding nonsense: exonic mutations that affect splicing. *Nat Rev Genet* **3:** 285–298

Charlet BN, Savkur RS, Singh G, Philips AV, Grice EA, Cooper TA (2002) Loss of the muscle-specific chloride channel in type 1 myotonic dystrophy due to misregulated alternative splicing. *Mol Cell* **10:** 45–53

Chen J, Kubalak SW, Chien KR (1998) Ventricular muscle-restricted targeting of the RXRalpha gene reveals a non-cell-autonomous requirement in cardiac chamber morphogenesis. *Development* **125:** 1943–1949

Chien KR (2000) Genomic circuits and the integrative biology of cardiac diseases. *Nature* **407:** 227–232

Estmer Nilsson C, Petersen-Mahrt S, Durot C, Shtrichman R, Krainer AR, Kleinberger T, Akusjarvi G (2001) The adenovirus E4-ORF4 splicing enhancer protein interacts with a subset of phosphorylated SR proteins. *EMBO J* **20:** 864–871

Faustino NA, Cooper TA (2003) Pre-mRNA splicing and human disease. *Genes Dev* **17:** 419–437

Fu X-D, Maniatis T (1990) Factor required for mammalian spliceosome assembly is localized to discrete regions in the nucleus. *Nature* **343:** 437–441

Fu X-D, Mayeda A, Maniatis T, Krainer AR (1992) General splicing factors SF2 and SC35 have equivalent activities *in vitro*, and both affect alternative 5′ and 3′ splice site selection. *Proc Natl Acad Sci USA* **89:** 11224–11228

Gomes AV, Guzman G, Zhao J, Potter JD (2002) Cardiac troponin T isoforms affect the Ca2 + sensitivity and inhibition of force development. Insights into the role of troponin T isoforms in the heart. *J Biol Chem* **277:** 35341–35349

Graveley BR (2000) Sorting out the complexity of SR protein functions. *RNA* **6:** 1197–1211

Gui JF, Lane WS, Fu X-D (1994) A serine kinase regulates intracellular localization of splicing factors in the cell cycle. *Nature* **369:** 678–682

Hanamura A, Caceres JF, Mayeda A, Franza Jr BR, Krainer AR (1998) Regulated tissue-specific expression of antagonistic pre-mRNA splicing factors. *RNA* **4:** 430–444

Hein S, Arnon E, Kostin S, Schonburg M, Elsasser A, Polyakova V, Bauer EP, Klovekorn WP, Schaper J (2003) Progression from compensated hypertrophy to failure in the pressure-overloaded human heart: structural deterioration and compensatory mechanisms. *Circulation* **107:** 984–991

Hodges D, Bernstein SI (1994) Genetic and biochemical analysis of alternative RNA splicing. *Adv Genet* **31:** 207–281

Hoffman BE, Lis JT (2000) Pre-mRNA splicing by the essential Drosophila protein B52: tissue and target specificity. *Mol Cell Biol* **20:** 181–186

Huang C, Zhou Q, Liang P, Hollander MS, Sheikh F, Li X, Greaser M, Shelton GD, Evans S, Chen J (2003) Characterization and *in vivo* functional analysis of splice variants of cypher. *J Biol Chem* **278:** 7360–7365

Huang TS, Nilsson CE, Punga T, Akusjarvi G (2002) Functional inactivation of the SR family of splicing factors during a vaccinia virus infection. *EMBO Rep* **3:** 1088–1093

Huang X, Pi Y, Lee KJ, Henkel AS, Gregg RG, Powers PA, Walker JW (1999) Cardiac troponin I gene knockout: a mouse model of myocardial troponin I deficiency. *Circ Res* **84:** 1–8

Jimenez-Garcia LF, Spector DL (1993) *In vivo* evidence that transcription and splicing are coordinated by a recruiting mechanism. *Cell* **73:** 47–59

Jumaa H, Wei G, Nielsen PJ (1999) Blastocyst formation is blocked in mouse embryos lacking the splicing factor SRp20. *Curr Biol* **9:** 899–902

Kanopka A, Muhlemann O, Petersen-Mahrt S, Estmer C, Ohrmalm C, Akusjarvi G (1998) Regulation of adenovirus alternative RNA splicing by dephosphorylation of SR proteins. *Nature* **393:** 185–187

Kovacic-Milivojevic B, Roediger F, Almeida EA, Damsky CH, Gardner DG, Ilic D (2001) Focal adhesion kinase and p130Cas mediate both sarcomeric organization and activation of genes associated with cardiac myocyte hypertrophy. *Mol Biol Cell* **12:** 2290–2307

Krawczak M, Reiss J, Cooper DN (1992) The mutational spectrum of single base-pair substitutions in mRNA splice junctions of human genes: causes and consequences. *Hum Genet* **90:** 41–54

Lemaire R, Prasad J, Kashima T, Gustafson J, Manley JL, Lafyatis R (2002) Stability of a PKCI-1-related mRNA is controlled by the splicing factor ASF/SF2: a novel function for SR proteins. *Genes Dev* **16:** 594–607

Lewandoski M, Wassarman KM, Martin GR (1997) Zp3-cre, a transgenic mouse line for the activation or inactivation of loxP-flanked target genes specifically in the female germ line. *Curr Biol* **7:** 148–151

Lindberg A, Kreivi JP (2002) Splicing inhibition at the level of spliceosome assembly in the presence of herpes simplex virus protein ICP27. *Virology* **294:** 189–198

Lokuta AJ, Meyers MB, Sander PR, Fishman GI, Valdivia HH (1997) Modulation of cardiac ryanodine receptors by sorcin. *J Biol Chem* **272:** 25333–25338

Longman D, Johnstone IL, Caceres JF (2000) Functional characterization of SR and SR-related genes in *Caenorhabditis elegans*. *EMBO J* **19:** 1625–1637

Mankodi A, Takahashi MP, Jiang H, Beck CL, Bowers WJ, Moxley RT, Cannon SC, Thornton CA (2002) Expanded CUG repeats trigger aberrant splicing of ClC-1 chloride channel pre-mRNA and hyperexcitability of skeletal muscle in myotonic dystrophy. *Mol Cell* **10:** 35–44

Maquat LE, Carmichael GG (2001) Quality control of mRNA function. *Cell* **104:** 173–176

Martone ME, Jones YZ, Young SJ, Ellisman MH, Zivin JA, Hu BR (1999) Modification of postsynaptic densities after transient cerebral ischemia: a quantitative and three-dimensional ultrastructural study. *J Neurosci* **19:** 1988–1997

Marx SO, Marks AR (2002) Regulation of the ryanodine receptor in heart failure. *Basic Res Cardiol* **97** (Suppl 1)**:** I49–I51

Mason JW (2002) Viral latency: a link between myocarditis and dilated cardiomyopathy? *J Mol Cell Cardiol* **34:** 695–698

Mayeda A, Screaton GR, Chandler SD, Fu XD, Krainer AR (1999) Substrate specificities of SR proteins in constitutive splicing are determined by their RNA recognition motifs and composite pre-mRNA exonic elements. *Mol Cell Biol* **19:** 1853–1863

Mermoud JE, Cohen PT, Lamond AI (1994) Regulation of mammalian spliceosome assembly by a protein phosphorylation mechanism. *EMBO J* **13:** 5679–5688

Misteli T, Spector DL (1998) The cellular organization of gene expression. *Curr Opin Cell Biol* **10:** 323–331

Nakai J, Imagawa T, Hakamat Y, Shigekawa M, Takeshima H, Numa S (1990) Primary structure and functional expression from cDNA of the cardiac ryanodine receptor/calcium release channel. *FEBS Lett* **271:** 169–177

Pasumarthi KB, Field LJ (2002) Cardiomyocyte cell cycle regulation. *Circ Res* **90:** 1044–1054

Ring HZ, Lis JT (1994) The SR protein B52/SRp55 is essential for Drosophila development. *Mol Cell Biol* **14:** 7499–7506

Sasik R, Calvo E, Corbeil J (2002) Statistical analysis of high-density oligonucleotide arrays: a multiplicative noise model. *Bioinformatics* **18:** 1633–1640

Schaal TD, Maniatis T (1999) Multiple distinct splicing enhancers in the protein-coding sequences of a constitutively spliced pre-mRNA. *Mol Cell Biol* **19:** 261–273

Schianffino S, Gorza L, Ausoni S (1993) Tropinic isoform switching in the developing heart and its functional consequences. *Trends Cardiovasc* **3:** 12–17

Sciabica KS, Dai QJ, Sandri-Goldin RM (2003) ICP27 interacts with SRPK1 to mediate HSV splicing inhibition by altering SR protein phosphorylation. *EMBO J* **22:** 1608–1619

Soonpaa MH, Kim KK, Pajak L, Franklin M, Field LJ (1996) Cardiomyocyte DNA synthesis and binucleation during murine development. *Am J Physiol* **271:** H2183–H2189

Toutant M, Costa A, Studler JM, Kadare G, Carnaud M, Girault JA (2002) Alternative splicing controls the mechanisms of FAK autophosphorylation. *Mol Cell Biol* **22:** 7731–7743

Towbin JA (1998) The role of cytoskeletal proteins in cardiomyopathies. *Curr Opin Cell Biol* **10:** 131–139

Townsend PJ, Barton PJ, Yacoub MH, Farza H (1995) Molecular cloning of human cardiac troponin T isoforms: expression in developing and failing heart. *J Mol Cell Cardiol* **27:** 2223–2236

Vellard M, Soret J, Sureau A, Perbal B (1991) A novel type of RNA-binding protein is potentially encoded by the opposite strand of the *trans*-spliced c-myb coding exon. *CR Acad Sci III* **313:** 591–597

Vercellotti GM (2001) Overview of infections and cardiovascular diseases. *J Allergy Clin Immunol* **108:** S117–S120

Wang HY, Xu X, Ding JH, Bermingham Jr JR, Fu X-D (2001) SC35 plays a role in T cell development and alternative splicing of CD45. *Mol Cell* **7:** 331–342

Wang J, Takagaki Y, Manley JL (1996) Targeted disruption of an essential vertebrate gene: ASF/SF2 is required for cell viability. *Genes Dev* **10:** 2588–2599

Zhang CL, McKinsey TA, Chang S, Antos CL, Hill JA, Olson EN (2002) Class II histone deacetylases act as signal-responsive repressors of cardiac hypertrophy. *Cell* **110:** 479–488

Zhang T, Maier LS, Dalton ND, Miyamoto S, Ross Jr J, Bers DM, Brown JH (2003) The deltaC isoform of CaMKII is activated in cardiac hypertrophy and induces dilated cardiomyopathy and heart failure. *Circ Res* **92:** 912–919

Zhou X, Marks PA, Rifkind RA, Richon VM (2001) Cloning and characterization of a histone deacetylase, HDAC9. *Proc Natl Acad Sci USA* **98:** 10572–10577

Zhou YY, Wang SQ, Zhu WZ, Chruscinski A, Kobilka BK, Ziman B, Wang S, Lakatta EG, Cheng H, Xiao RP (2000) Culture and adenoviral infection of adult mouse cardiac myocytes: methods for cellular genetic physiology. *Am J Physiol Heart Circ Physiol* **279:** H429–H436